Geomechanics and Engineering, *Vol. 8, No. 6 (2015) 811-828*
DOI: http://dx.doi.org/10.12989/gae.2015.8.6.811

Flow models of fluidized granular masses with different basal resistance terms

Hengbin Wu [*1,2], Yuanjun Jiang [3] and Xuefu Zhang [2]

[1] *College of Civil Engineering, Chongqing Three Gorges University, Chongqing, China*
[2] *State Key Laboratory Breeding Base of Mountain Bridge and Tunnel Engineering, Chongqing Jiaotong University, Chongqing, China*
[3] *Key Laboratory of Mountain Hazards and Earth Surface Processes, Institute of Mountain Hazards & Environment, Chinese Academy of Sciences, Chengdu, China*

(*Received September 01, 2014, Revised February 07, 2015, Accepted February 14, 2015*)

Abstract. Proper modelling of the basal resistance terms is key in simulating the motion of fluidized granular flow. In this paper, standard depth-averaged governing equations of granular flow are used together with the classical Coulomb, Voellmy, and velocity dependent friction models (VDFM). A high-resolution modified TVDLF method is implemented to solve the partial differential equations without numerical oscillations. The effects of basal resistance terms on the motion of granular flows such as geometric shape evolution, travel times and final deposits are analyzed. Based on the numerical results, the predictions of the front and rear end positions and developing length of granular flow with Coulomb friction model show excellent agreements with experiment results reported by Hutter *et al.* (1995), and illustrate the validity of the numerical approach. For the Voellmy model, the higher value of turbulent coefficient than reality may obtain more reasonable predicted runout for the small-scale avalanche or granular flow. The energy exchange laws indicate that VDFM is different from the Coulomb and Voellmy models, although the flow characteristics of both three models fit the measurements and observations very well.

Keywords: granular flow; avalanche dynamics; basal resistance terms; deposition process

1. Introduction

Granular flows are widely used in the civil and mechanical engineering and material science. One of the very first and systematic theoretical models was proposed by Bagnold (1954) for neutrally buoyant suspension of particles. In recent years, granular flows have been applied to simulate the hazardous motions of landslides, debris flows, debris avalanches and mud flows. The simulation methods of granular flow are of two kinds: continuum model, so-called the computational fluid dynamics, and non-continuum, or discrete models (Teufelsbauer *et al*. 2011, Li *et al*. 2012, Chen *et al*. 2012, 2013a, b). Savage and Hutter (1989) proposed, perhaps, the first incompressible frictional granular flow equations in the form of the depth-averaged mass and momentum balance equations along the sliding surface. These models have been successively extended to higher complexities, in geometric and mechanics (see, e.g., Gray *et al*. 1999, Tai *et al*.

*Corresponding author, Ph.D., E-mail: hbw8456@163.com

http://www.techno-press.org/?journal=gae&subpage=7 ISSN: 2005-307X (Print), 2092-6219 (Online)

2002, Pudasaini and Hutter 2007, Fischer *et al*. 2012). These models are widely and successfully used in the numerical simulation of landslides, granular flows, avalanches and debris flows.

Savage-Hutter-type models have been successively extended to include the aspects of pore pressure (Iverson 1997, Iverson and Denlinger 2001, Pudasaini *et al*. 2005a, b), complex terrain (Pudasaini *et al*. 2005a, Fischer *et al*. 2012), erosion and entrainment (Pitman *et al*. 2003, Tai and Kuo 2008), earth pressure coefficient (Pudasaini and Kröner 2008), and numerical algorithm with high resolution (Tai *et al*. 2002, Pudasaini and Hutter 2007). The original Savage-Hutter model is suitable for dry granular flow. Iverson (1997) considered the effects of pore pressure in the debris mixture flow, and extended the Coulomb model to the Coulomb mixture flow. This model has been further extended later (Iverson and Denlinger 2001, Pudasaini *et al*. 2005a). Nevertheless, Iverson (1997) and Iverson and Denlinger (2001) models are based on the ad-hoc decomposition of the total basal load into the solid and fluid components, by introducing a decomposition variable (λ). This new internal variable later required an extra closure, which led Iverson and Denlinger (2001) to the introduction of an extra advection-diffusion equation. Although their model has been able to capture certain aspects of the debris mixture, their model lacks the physics of flow of a two-phase debris material. The main drawback in their model originates from the assumption that the solid velocity equals the fluid velocity which may not be the valid criterion in general. Because, this effectively prevents the evolution of the pore pressure in the mixture, drag cannot be generated, no phase-interactions could be included, and that their model is effectively a single-phase model (Pitman and Le 2005, Pudasaini *et al*. 2005a, Fernández-Nieto *et al*. 2008, Hutter and Schneider 2010). By proposing a two-fluid model, Pitman and Le (2005) included the simple and linear drag force between solid phase and liquid phase into the governing equations. But their model does not include the viscous shear effects of the fluid.

Recently, several key and new physical aspects of a real two-phase debris flow have been presented by Pudasaini (2012) by introducing the virtual mass force that emerges from the fact that the solid phase could accelerates relative to the liquid phase as the debris flows. This enhances the kinetic energy of the ambient fluid due to the accelerating particles. Similarly, other aspects included in the general two-phase debris mass flows (Pudasaini 2012) are: buoyancy, enhanced non-Newtonian viscous stress as modelled by including the solid-volume fraction gradient in the mixture, and the usual Newtonian viscous effects. Another important aspect is the generalized drag, which includes both the solid-like and fluid-like drags and all spectrum connecting these limiting states. Further, the generalized drag includes both the linear and quadratic effects in the flow. This way, the general two-phase debris flow model (Pudasaini 2012) reveals strong interactions between the solid- and liquid-phase. This model has been further extended and applied to different flow scenarios, including the tsunami generated by the subaerial and submarine landslides, and their complex dynamics (Pudasaini 2014), and the rock-ice avalanches, as described by a new enhanced mechanical model (Pudasaini and Krautblatter 2014).

As in the shallow water equations, the depth-averaged equations for granular flow are derived by integrating the mass and momentum balance equations along the flow depth resulting in the mass and momentum balances in the surface parallel direction in which the field variables are the depth-averaged velocities and the flow height (Savage and Hutter 1989, Camassa and Holm 1993, Pudasaini and Hutter 2007). But, there are several significant differences between these two models: (1) The forces due to the complex terrain that are included in the granular flow models are more complicated than shallow water equations in which such forces are typically ignored (Gray *et al*. 1999, Pudasaini *et al*. 2005a, Fischer *et al*. 2012); (2) The influences of erosion and entrainment to the motion are more significant (Pitman *et al*. 2003, Tai and Kuo 2008). (3) The

shear stresses in granular material is proportional to normal stress, and the friction coefficient, and anisotropic stress distributions (Savage and Hutter 1989). A detailed and comprehensive description on these important aspects of granular flows and avalanches can be found in Pudasaini and Hutter (2007).

In hydraulics, it is commonly assumed that the pressure within the flowing sheet is hydrostatically distributed, the assumption of hydrostatic stress distribution is reasonable for fluids and unrealistic for granular materials with internal strength (Hungr 2008). Present models of the earth pressure coefficient have three types: Savage-Hutter model (Savage and Hutter 1989), Rankine model (Wang *et al*. 2010, Hungr 2008), and improved Savage-Hutter model (Hungr and McDougall 2009).

We also mention that, recently, Domnik and Pudasaini (2012) and Domnik *et al*. (2013) presented novel pressure- and rate-dependent Coulomb-viscoplastic flow models, and multiscale and efficient simulation techniques to describe the full dynamics of the granular flow from initiation to the final depositions. Their unified modelling and simulation technique includes all the basic features of the granular flow, which at the same time is very fast due to the coupling between the full-dimensional and depth-averaged models with the proper domain decomposition. These advanced models do not use hydrostatic assumption, rather a full dynamic pressure is computed that is very important in proper modelling of complex flows during the mass collapse, flow obstacle interactions, and also in the depositions.

Basal resistance terms play an important role and significantly influence the flow characteristics in the motion of granular flow. There is variety of forms of basal resistance terms in granular flows. In the present study, our goal is to analyze the effects of some of them to the motion for granular flows, such as geometric shape evolution, runout distance and velocity distribution, a detailed analysis has been presented. Numerical results are compared for three different basal resistance terms and the conclusions are drawn.

2. Mathematical model of granular flow

2.1 Governing equations

As shown in Fig. 1, we build the slope fitted coordinate system in which x points in the down-slope direction, y points in the cross-slope direction, and z points in the vertical direction. Typical granular flows such as landslides, debris flows and avalanches, can be described by incompressible frictional granular flow equations consisting of the mass and momentum balance equations, in which the flow mechanics is described by Mohr-Coulomb-type (or other suitable) models (Savage and Hutter 1989, Pudasaini and Hutter 2007). Assuming that granular flow is incompressible and of constant density, the governing equations can be given by

$$\frac{\partial h}{\partial t}+\frac{\partial (hu)}{\partial x}=0, \tag{1}$$

$$\frac{\partial (hu)}{\partial t}+\frac{\partial (hu^2)}{\partial x}=gh\sin\theta-\frac{u}{|u|}gh\tan\delta(\cos\theta+\lambda\kappa u^2)-\frac{1}{2}gk_{ap}\frac{\partial}{\partial x}(\cos\theta h^2), \tag{2}$$

where h and u are height and depth averaged velocity of granular, respectively. θ and δ denote

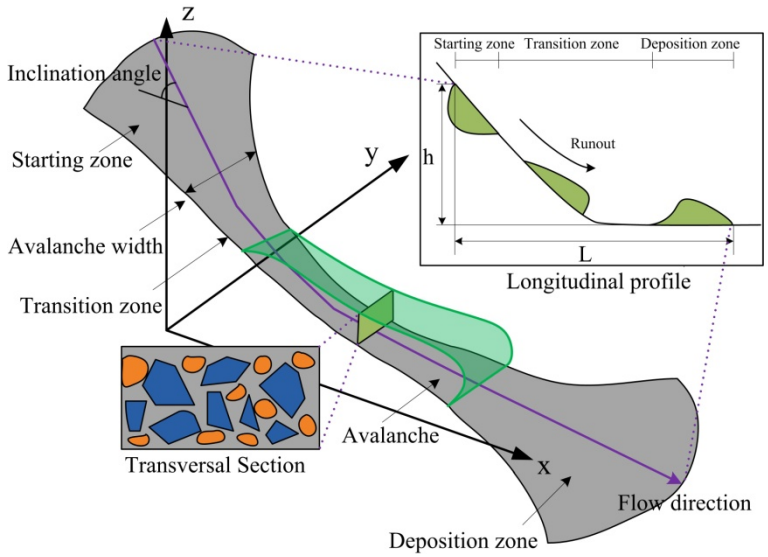

Fig. 1 Sketch of granular flow, the flow zones can be divided into three: starting zone, transition zone, and deposition zone. The details of transversal and longitudinal profile are shown in the lower left part and upper right part, respectively

inclined angle and basal Coulomb dry-friction angle, respectively. $\lambda\kappa$ denotes local radius of curvature of the master curve. k_{ap} represents ratio of the normal stress to the lateral one, we follow Savage and Hutter (1989), it can be written as

$$k_{ap} = 2\sec^2\phi_{\text{int}}\left(1 \mp \sqrt{1-\cos^2\phi_{\text{int}}\sec^2\delta}\right) - 1, \tag{3}$$

where the + applies when flow is converging (passive state), and the – applies when flow is elongating (active state); ϕ_{int} denotes internal friction angle.

For quasi-static deformation this coefficient can be calculated from the standard Mohr-Coulomb plasticity model, as was done by Savage and Hutter (1989). Pouliquen and Forterre (2002) proposed that for dense granular flows on rough surfaces, the material behaves more like a fluid, numerical results tend to show that the vertical and horizontal normal stresses are anisotropic. Nevertheless, Pudasaini and Kröner (2008) showed that the deposition process is strongly and requires earth pressure coefficient other than unity. Two types of the earth pressure coefficients mentioned above are used in the numerical simulation of granular flow and discussed in the following numerical simulations.

To properly model the effect of the changing topography, we apply the curvatures of the basal topography as in Gray *et al*. (1999). The more general form that substantially improves the dynamics by enhancing, e.g., the Coulomb friction, gravity and pressure gradients, can refer to Pudasaini *et al*. (2005a), Fischer *et al*. (2012).

2.2 Basal resistance terms

The momentum equations of granular flow have five parts: mass flux over time, momentum

flux, hydraulic pressure gradient, driving gravitational force, and dissipative basal friction force. The basal and internal friction angles are obtained from laboratory tests of material, and further applied in the natural rock avalanche, landslide and debris flow. Real flows often involve a mixture of solid materials and fluids, a rheology that is usually difficult to characterize but certainly require more complex models to capture the effect of fluidizations. In this paper, three present single-phase models including Coulomb, Voellmy and VDFM are described and employed in the numerical simulations.

Coulomb model

The classic Coulomb friction law proposed by Savage and Hutter (1989) indicates that the shear stress is proportional to the normal stress at the base, and the coefficient of friction is a constant. The basal resistance term of Coulomb model can be written as

$$\tau_b = -\frac{u}{|u|}\rho g h \cos\theta \tan\delta. \tag{4}$$

Voellmy model

The two parameters model was developed for use in lump mass modeling of snow avalanches, and a major modifications was made by Salm (1993). Voellmy model has two parts: friction and turbulence terms. Friction term is represented by friction coefficient that is similar with the Coulomb model; while, the turbulence term represents the basal friction effects. Voellmy model can be given by

$$\tau_b = -\frac{u}{|u|}\left(\rho g h \cos\theta \tan\delta + \rho g \frac{u^2}{\xi}\right), \tag{5}$$

where ξ is turbulent coefficient accounting for velocity-dependent friction losses. In the context of landslide dynamics and the equivalent fluid approach, the second term is not included to account for either air drag or turbulence, alone, but rather to empirically account for all eventual sources of velocity-dependent resistance (Chen and Lee 2003). Nevertheless, as mentioned in Fischer *et al*. (2012), the Voellmy-type model is not physically fully justified.

Velocity dependent friction model (VDFM)

For the flow of granular material on rough surfaces and for moderate inclinations, experiments based on spherical glass beads with friction angle close to the slope angle reveal a more complex behavior, the onset of flow depends both on the inclination of the plane and on the thickness of the granular layer, the simple Coulomb friction law cannot capture the features. An empirical friction law based on scaling properties measured for steady uniform flows was proposed by Pouliquen (1999a, 1999b) and further improved by Pouliquen and Forterre (2002) and Johnson and Gray (2011).

For the glass beads used in the experiments, an initially static granular layer starts to flow when the inclination reaches a critical value $\theta_{start}(h)$; to stop the flow, we have to decrease the inclination to a lower angle $\theta_{stop}(h)$. $\mu_{start}(h)$ and $\mu_{stop}(h)$ are the tangent of two critical angle mentioned above and given by fitting the measured experiments data

$$\mu_{start}(h) = \tan\delta_1 + (\tan\delta_2 - \tan\delta_1)\frac{1}{h/L+1}, \tag{6}$$

$$\mu_{stop}(h)=\tan\delta_3+\left(\tan\delta_2-\tan\delta_1\right)\frac{1}{h/L+1}, \tag{7}$$

where δ_1, δ_2, δ_3 denote friction angles; the parameter L, which has the dimensions of length, depends on the granular material and surface properties of the plane and characterizes the depth of flow over which a transition between the two friction angle occurs (Johnson and Gray 2011).

The expressions for the friction coefficient ($\mu(h, Fr)$) can be written as follows in terms of the thickness h and the local Froude number $Fr=\frac{\|u\|}{\sqrt{gh}}$

$$\mu(h,Fr)=\begin{cases}\mu_{stop}\left(h\dfrac{\beta}{Fr}\right) & if\ Fr>\beta\\ \mu_{start}(h)+\left(\mu_{stop}(h)-\mu_{start}(h)\right)\cdot\left(\dfrac{Fr}{\beta}\right)^{\gamma} & if\ \beta>Fr>0,\\ \min\left(\mu_{start}(h),\left|\tan\theta-k_{ap}\dfrac{\partial h}{\partial x}\right|\right) & if\ Fr=0\end{cases} \tag{8}$$

where β and γ are measurement constants. Nevertheless, physically correct Froude number should include the factor $\cos\theta$, pressure and gravitational potential energy as explained in Pudasaini and Domnik (2009) and Domnik and Pudasaini (2012) with extended and generated Froude numbers. The extended Froude number for depth-averaged flows is defined as the ratio between the kinetic and the potential energy

$$Fr=\frac{\|u\|}{\sqrt{ghk_{ap}\cos\theta+g\sin\theta\left(x_d-x\right)}}, \tag{9}$$

where, x_d is the constant of integration, which is the distance from the point of the mass release along the channel to the point where the flow hits the horizontal reference datum.

To easily employ Eq. (8) in the governing equations of granular flow, the friction coefficient can be transferred into the form of basal shear stress. With the velocity dependent friction coefficient Eq. (8), the basal shear stress Eq. (4) reduces to, (because $\tan\delta=\mu$)

$$\tau_b=-\frac{u}{|u|}\rho gh\cos\theta\cdot\mu(h,Fr). \tag{10}$$

3. Numerical approach

In order to test the above model equations (mention Eqs. (1)-(2)) against avalanche events either in nature or in the laboratory, a numerical integration scheme must be constructed (Pudasaini and Hutter 2007, Pitman *et al*. 2003, Savage and Hutter 1991). In the past decades, numerical techniques have been developed to solve the Savage-Hutter avalanche equations for typical moving boundary value problems of granular flows (Pudasaini and Hutter 2007). Early attempts used Lagrangian moving mesh finite difference schemes (Savage and Hutter 1989, 1991,

Hutter *et al*. 1995) and traditional Eulerian integration techniques (Savage and Hutter 1989, Pudasaini and Hutter 2007) are susceptible to numerical instabilities and cause non-physical oscillations in regions of large gradients of the variables. Shock capturing finite difference techniques (Pudasaini and Hutter 2007, Ouyang *et al*. 2013) and Godunov-type finite volume methods (Denlinger and Iverson 2001, Toro 2001, Pitman *et al*. 2003) were applied, respectively. We choose a recently developed high-resolution approach, namely the modified total variation diminishing Lax-Friedrichs (MTVDLF) type difference method. The governing equations of granular flow can be rewritten as follows

$$\begin{aligned} &\frac{\partial U}{\partial t}+\frac{\partial F(U)}{\partial x}=S(U), \\ &U=\begin{bmatrix} h \\ hu \end{bmatrix}, \quad F(U)=\begin{bmatrix} hu \\ hu^2+\frac{1}{2}k_{ap}gh^2\cos\theta \end{bmatrix}, \quad S(U)=\begin{bmatrix} 0 \\ g\sin\theta h-\frac{u}{|u|}\rho gh\cos\theta\tan\delta \end{bmatrix}. \end{aligned} \tag{11}$$

A transformation of Eq. (10) is given by

$$\begin{aligned} &\frac{\partial U}{\partial t}+A(U)\frac{\partial U}{\partial x}=S(U), \\ &A(U)=\frac{\partial F(U)}{\partial U}=\begin{bmatrix} 0 & 1 \\ -u^2+k_{ap}gh\cos\theta & 2u \end{bmatrix}. \end{aligned} \tag{12}$$

The original TVDLF method of Yee (1989) was extended and improved by Tóth and Odstrčil (1996). This method has been verified to solve the granular gravity driven free surface flows (Thornton 2005). They introduced the Hancock predictor step to increase the temporal accuracy, and suggested that Yee's original anti-diffusive flux should be multiplied by a local or global Courant number to obtain a less diffusive scheme. The Hancock predictor step is used to calculate $U_j^{n+1/2}$ with a second-order accurate in space as well as time

$$U_j^{n+1/2}=U_j^n-\frac{\Delta t}{2\Delta x}\left\{F\left(U_{j+1/2}^n\right)-F\left(U_{j-1/2}^n\right)\right\}+\frac{\Delta t}{2}S_j^n. \tag{13}$$

All the variables and fluxes are obtained, and then a full step, using this predictor half step, as follows

$$U_j^{n+1}=U_j^n-\frac{\Delta t}{\Delta x}\left\{F^{MLF}\left(U_{j+1/2}^{n+1/2}\right)-F^{MLF}\left(U_{j-1/2}^{n+1/2}\right)\right\}+\Delta t S_j^n. \tag{14}$$

We mention that these flows may better be simulated by using other numerical methods, such as, TVD-NOC (Tai *et al*. 2002). However, this is subject to scrutiny with experimental or field data. For more detail on it, we refer to Pudasaini and Hutter (2007).

4. Numerical experiment

A series of laboratory experiments were carried out by Hutter *et al*. (1989), and further reported by Savage and Hutter (1991). Experiment No. 87 (see Hutter *et al*. 1989, 1995) involving flow of

1500 g of particles down a bed lined with drawing paper and having an initial inclination of 50° is implemented in the paper (see Fig. 2). Experiments were performed in a 100 mm wide chute made up of two straight portions (one inclined of 1,700 mm length and the other horizontal 1,700 mm long) connected by replaceable circular arc sections (246 mm radius). The granular materials employed Vestolen plastic particles, with a mean diameter of 3.5 mm, bulk density of 540 kg/m^3, and the drawing paper was adopted in the bed lining to simulate the basal friction (see Table 1). The main aspect of this paper is to simultaneously study and analyze the effect of different basal friction laws on the dynamics, run-out, and deposition of fluidized granular flows down a one-dimensional curved basal topography that merges into a horizontal run-out.

4.1 Numerical results for Coulomb model

Four cases of Coulomb model are performed in the analysis (see Table 2), three values of bed friction angle (20°, 21.5° and 23°) and two values of internal friction angle (25° and 29°) are adopted to analyze their effects on the dynamic characteristics of granular flow. The numerical results have been scaled by L_0 for length, H_0 for height (depth), $\sqrt{L_0 g}$ for velocity and $\sqrt{L_0 / g}$ for time, respectively.

Fig. 3 shows the experimental measurements and theoretical predictions of the evolution of the leading and trailing edge positions of the granular avalanche. It can be seen that the moving time and runout distance decrease with increasing bed friction angle, and are fairly insensitive to the value of the internal friction angle; this arguments coincide with the conclusions drawn by Hutter *et al*. (1989, 1995). The numerical results of Coulomb-2 with a δ of 21.5° and ϕ_{int} of 29° show excellent agreement in terms of the front and rear end positions of the moving mass in line with the findings by Hutter *et al*. (1989, 1995). We can conclude that the numerical approach adopted in

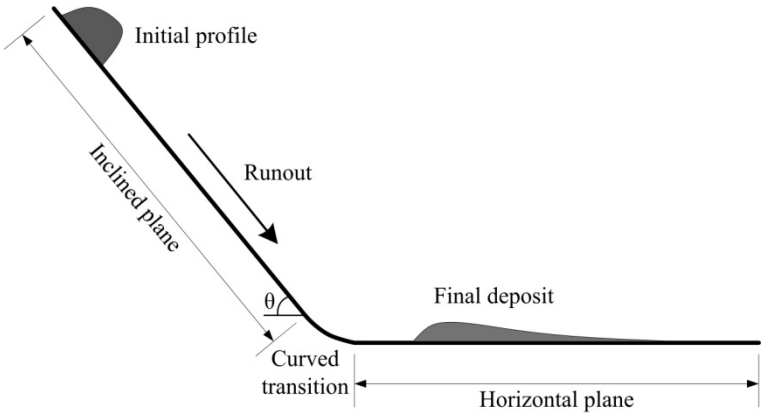

Fig. 2 Sketch of channel geometry in the numerical simulations

Table 1 Conditions and material parameters in the laboratory experiments (m denotes granular mass; L_0, H_0 are initial length and height of granular flow, respectively)

Parameters	m (g)	ρ (kg/m^3)	L_0 (mm)	H_0 (mm)	θ (°)
Value	1,500	540	300	150	50

Table 2 Physical parameters and numerical results of Coulomb model

Run No.	δ (°)	ϕ_{int} (°)	Travel time ($\sqrt{L_0/g}$)	Runout distance (L_0)
Coulomb-1	20	29	9.33	11.36
Coulomb-2	21.5	29	8.77	10.71
Coulomb-3	23	29	8.31	10.19
Coulomb-4	21.5	25	8.75	10.83

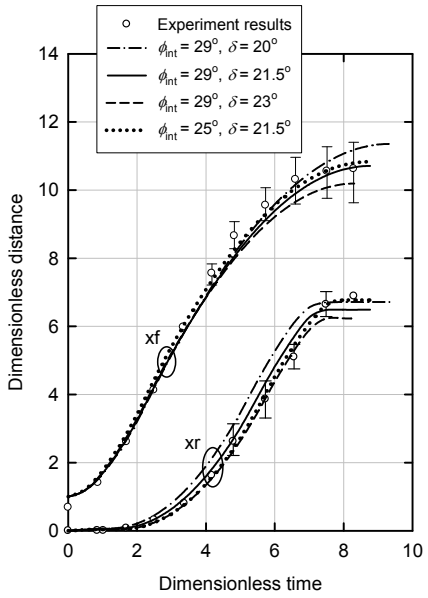

Fig. 3 Experimental measurements and theoretical predictions of the evolution of the leading (*xf*) and trailing (*xr*) edge positions of the granular avalanche; ϕ_{int} and δ denote internal friction angle and bed friction angle of granular materials, respectively. Circle symbols represent experiment results of Vestolen avalanches reported by Hutter *et al*. (1989, 1995)

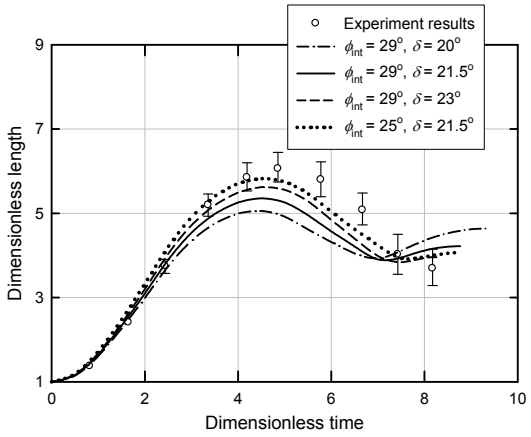

Fig. 4 Comparisons of the developing length of moving mass of experiment and numerical results

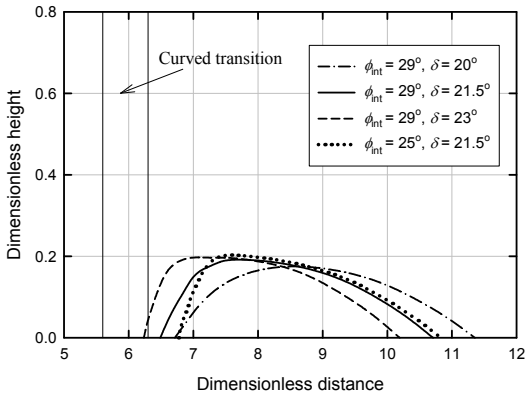

Fig. 5 Final deposits for Coulomb model

the paper is suitable and numerical results are realistic and reliable.

Fig. 4 shows the developing length of the moving mass, circle symbols represent experiment results reported by Savage and Hutter (1991) and Hutter *et al*. (1995). From Fig. 4, we see that the predictions of the accelerating phase is more accurate than that of the decelerating phase, and the final deposits are conformed with measurement results. In addition, the developing length of granular material increases with increasing bed friction angle, and decreases with increasing internal bed friction; the internal friction angle has significant effects on the dimensionless length of granular, because it can influence the earth pressure coefficient and flow profile (see Pudasaini and Kröner 2008 for more details). Table 3 illustrates the earth pressure coefficients with different material parameters, the active and passive earth pressure coefficients depend on whether an element of material is being elongated or compressed in the direction parallel to the bed.

Table 3 Earth pressure coefficients of Coulomb model with different granular material parameters (k_a and k_p denote active and passive values of earth pressure coefficient, respectively)

Run no.	δ (°)	ϕ_{int} (°)	k_a	k_p
Coulomb-1	25	21.5	0.88	1.99
Coulomb-2	29	20	0.66	2.5
Coulomb-3	29	21.5	0.72	2.51
Coulomb-4	29	23	0.80	2.43

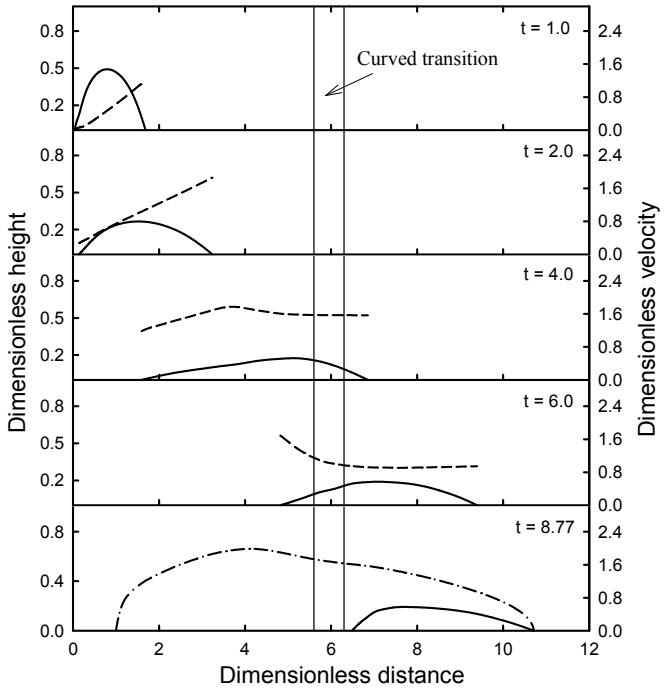

Fig. 6 Flow characteristics of granular materials at five different dimensionless times for Coulomb-3 case. The solid, dot and dash-dot (last panel) lines denote flow profile, velocity distribution and front velocity of granular flow, respectively

The final deposits of four cases are shown in Fig. 5, we see that the final deposits tend to be thin fronts and thick rear ends for the Coulomb friction law (Pudasaini *et al*. 2005a), it is actually reported in some of landslide and rock avalanches, but generally the actual debris distribution shows the opposite trend (Hungr and Evens 1996). It is reasonable for using the typical Coulomb friction law to describe the flow characteristics of homogeneous granular material, but the real events such as natural rock avalanche and landslide are more complex and difficult to capture the effect of fluidization, which is not within the scope in the paper. In addition, it is also seen that the final deposits have a steeper rear end with increasing bed friction angle and decreasing internal friction angle.

The granular flow characteristics at five different dimensionless times (t = 1.0, 2.0, 4.0, 6.0 and final time) for Coulomb-3 case are shown in Fig. 6. We see that the granular mass starts to move due to the gravity and hydraulic pressure gradient, the velocities of granular material in the inclined plane vary almost linearly (t = 1.0 and 2.0), it ensures the symmetric flow profile during the motion if the initial flow profile is symmetric (Tai *et al*. 2002). When the front end of granular material reaches the curved section, the velocity decreases in the approaching front. Finally, the granular mass reaches the horizontal section. Then, first the head of granular material begins to settle. The approaching granular material from the upslope impacts the already deposited granular hip. The maximum runout distance and runout time for the Coulomb model are about 8.77 and 10.71, respectively. These phenomena are in line with those already described in Pudasaini *et al*. (2005a), and Pudasaini and Hutter (2007). In conclusion, the modified TVDLF method gives good predictions of the dynamic characteristics of granular flow with experiment results.

4.2 Numerical results for Voellmy model

Compared with the classic Coulomb friction law, Voellmy model has two parts, a dry-Coulomb type friction and a velocity squared drag. This model has been widely applied in the simulation of mass movements, especially for granular avalanches. Three cases with different turbulent coefficients are performed in the analysis, and the material parameters and numerical results are shown in Table 4. The numerical results of Voellmy model is shown in Fig. 7. It can be seen that the front and rear end positions increase with increasing turbulent coefficient, and the rear end positions are smaller than that of Coulomb model due to the Voellmy drag. Voellmy drag moderately influences the leading edge positions, but significantly influences the trailing edge positions perhaps due to the value range of turbulent coefficients chosen in the numerical simulations. The predicted runout distance and moving time increase with increasing turbulent coefficient, Voellmy-3 case with a turbulent coefficient of 2000 m/s^2 shows excellent agreement with the experiment results.

For the original Voellmy model, friction part is dependent on the geometric shape, and independent on the granular materials; the turbulent coefficient depends on the turbulent friction

Table 4 Physical parameters and numerical results of Voellmy model

Run No.	δ (°)	ϕ_{int} (°)	ξ (m/s^2)	Travel time ($\sqrt{L_0/g}$)	Runout distance (L_0)
Voellmy-1	21.5	29	500	8.60	9.84
Voellmy-2	21.5	29	1200	9.17	10.89
Voellmy-3	21.5	29	2000	9.22	11.06

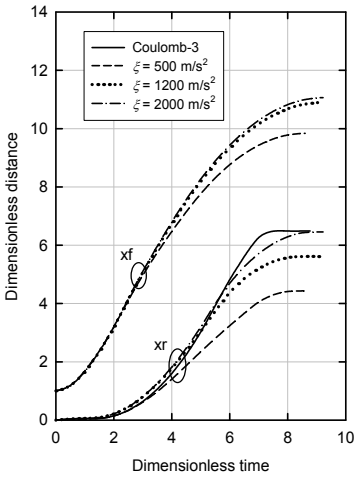

Fig. 7 Numerical results of the evolution of the leading and trailing edge positions of the granular avalanche with Voellmy model

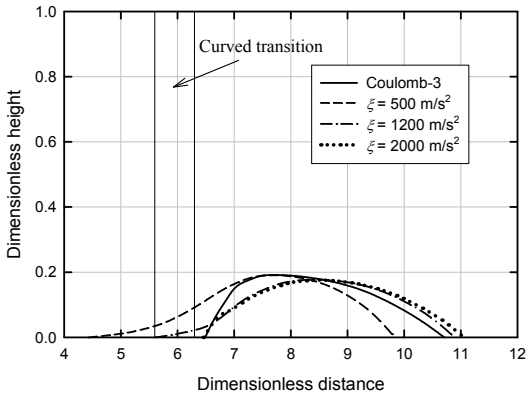

Fig. 8 Final deposits for voellmy model

(Fischer *et al*. 2012). Pudasaini and Hutter (2007) found this notion conflicts the observations by experiment and large-scale landslide. Salm (1993) interpreted the turbulent coefficient as a viscous friction, and the value of ξ mainly depends on the topography. Fig. 8 shows the final deposits of several Voellmy model cases, the predictions of Voellmy model elongate the final deposits than that of Coulomb model. According to the observed data by Chen and Lee (2003), Fischer *et al*. (2012) and Hungr and Evans (1996), the turbulent coefficient ranges from 100 to 1,000 m/s^2 (range from 200 to 300 m/s^2 for coalmine waste dump failures, range from 500 m/s^2 for rock avalanches). However, the case of Voellmy-3 with a ξ of 2000 m/s^2 shows excellent agreement with the predicted results for Coulomb model. We can conclude that the higher value of turbulent coefficient than reality may obtain more reasonable predicted runout for the small-scale avalanche or granular flow.

4.3 Numerical results for VDFM

The material parameters of VDFM are obtained by fitting the empirical data, our goal in the analysis is not to find the parameter combination that best fits the measurements and observations. This can easily be achieved with all three models. Instead we want to analyze the sensitivity of dynamic characteristic to material parameters with different basal resistance terms. Referring Pouliquen (1999a, b), the friction angles are chosen as $\delta_1 = 21°$, $\delta_2 = 30.7°$, $\delta_3 = 2.22°$; $\beta = 0.136$ denotes a measured constant for glass beads; γ is chosen equal to 10^{-3}, because the predictions of the model are not sensitive to its value as long as γ is less than 10^{-2} (Pouliquen and Forterre 2002). $L = 0.65$ provides a convenient length scale with which to non-dimensionalise the depth of the flow (Johnson and Gray 2011). Three cases of VDFM are performed in this analysis and the material parameters are shown in Table 5.

Fig. 9 shows the numerical results of the evolution of the front and rear end positions of the granular avalanche with VDFM. It is known that the front and rear end positions of VDFM are much smaller than that of Coulomb model, because the material parameters adopted in the numerical

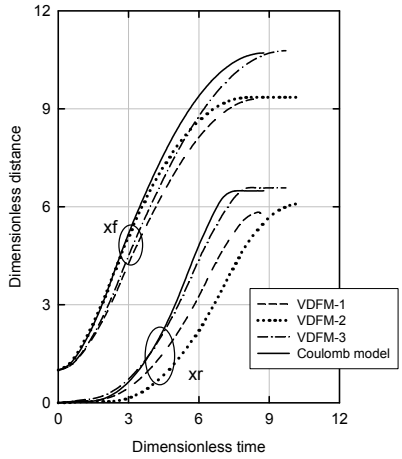

Fig. 9 Numerical results of the evolution of the leading and trailing edge positions of the granular avalanche with VDFM

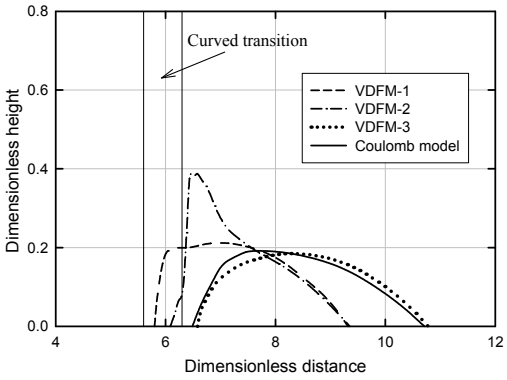

Fig. 10 Final deposit for VDFM

Table 5 Physical parameters and numerical results of VDFM (S-H denotes the earth pressure coefficient employs the Savage-Hutter assumption)

Run No.	δ_1 (°)	δ_2 (°)	δ_3 (°)	β	L (mm)	k_{ap}	Travel time ($\sqrt{L_0/g}$)	Runout distance (L_0)
VDFM-1	21	30.7	22.2	0.136	0.65	S-H	8.64	9.32
VDFM-2	21	30.7	22.2	0.136	0.65	1.0	10.24	9.35
VDFM-3	18.0	26.0	19.0	0.136	0.65	S-H	9.71	10.78

analysis are taken from glass beads, and different with Vestolen in experiment conducted by Hutter *et al*. (1995). We further analyze the effect of earth pressure coefficient on the dynamic characteristics of granular flow. The isotropic conditions i.e., earth pressure coefficients equal 1.0, are implemented to analyze the effect of earth pressure coefficient on the flow characteristics. Fig. 9 indicates that the runout distances are very close, while the moving time of hydrostatic assumption is longer than that of Savage-Hutter assumption.

Fig. 10 indicates that the runout distances with hydrostatic assumption and Savage-Hutter assumption are very close. Nevertheless, there have significant differences between two models, the rear end with hydrostatic assumption has a larger thickness than that with Savage-Hutter assumption. We can conclude that the effect of earth pressure coefficients on the motion of granular flow cannot be ignored even for VDFM in line with findings by Pudasaini and Kröner (2008). For the details of more pressure assumption models, we can refer to Pirulli *et al*. (2007) and Hungr and McDougall (2009).

5. Energy in granular flows

Typical granular flow involves complex energy exchange (for detailed description, see Pudasaini and Domnik 2009, Domnik and Pudasaini 2012). The potential energy, E_p, is transferred

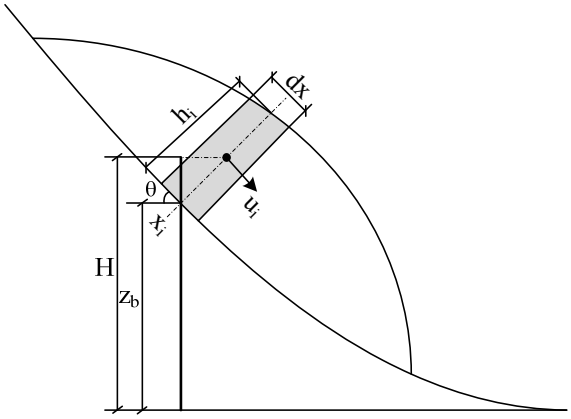

Fig. 11 Sketch of calculating energy of granular cells. We assume that each cell of granular has a uniform height, and the potential energy can be obtained by the gravity center of granular cell

to the kinetic energy, E_k, and the friction induced internal energy E_f, when granular materials are released on the inclined plane. The total energy of granular materials is the summary of potential, kinetic and friction induced internal energy, $E_t = E_p + E_k + E_f$. To simplify the analysis, and the losses of the potential and kinetic energy represent the dissipative energy that is induced by the basal friction force. Based on the conclusions reported by Fei *et al*. (2010), the width of chute (W_0) is considered, the kinetic and potential energies are given by

$$E_k = 0.5 \cdot mu^2 = \sum_i E_k = \rho g H_0 L_0^2 W_0 \sum_i 0.5 \cdot h_i u_i^2 dx, \tag{15}$$

$$E_p = mgH = \sum_i E_p = \rho g H_0 L_0 W_0 \sum_i \left(z_b + 0.5 \cdot h_i \cos\theta\right) h_i dx, \tag{16}$$

where E_k, E_p denote kinetic and potential energies, respectively; h_i, u_i are height and zelocity of each granular cell, dx denotes the length of granular cell. Noting that the zero of potential energy locates in the horizontal plane, and the height of the basal topography (z_b) can be directly obtained.

Fig. 12 illustrates the energy exchange laws during the motion of granular materials. Kinetic and potential energies are obtained by using Eqs. (15)-(16). We assume that the energy losses during the motion caused by the basal friction force, and the complex flow behavior such as rolling and collisions between multi-contact particles are ignored. Thus, the dissipative energy can be deduced by the decreases of total mechanical energy. From Fig. 13, we see that when granular mass starts to move, the kinetic energy increases and potential energy decreases because the developing length increases and corresponding height decreases. When the rear end of granular material reaches the horizontal plane, the potential energy is very small, because the zero potential datum locates the horizontal plane. It is worth noting that the energy exchange laws for Coulomb and Voellmy models are very close, the kinetic and dissipative energies of VDFM are smaller compared with the other models.

Fig. 13 is the energy change rates ($\Delta E / \Delta t$) during the motion of granular materials with

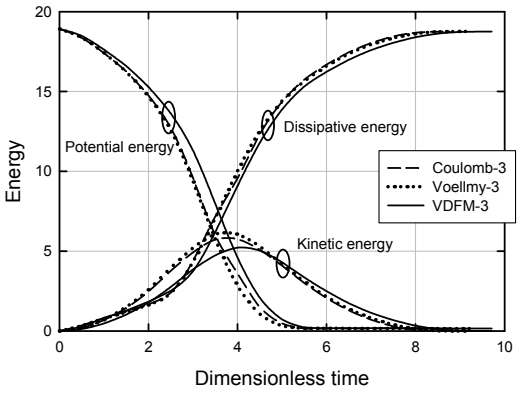

Fig. 12 Energy exchange laws during the motion of granular flow with three different basal resistance terms

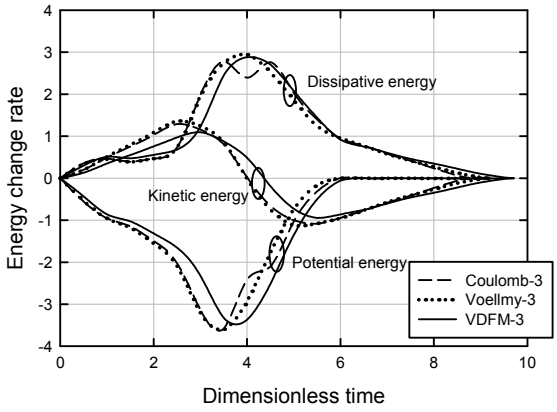

Fig. 13 Energy change rates during the motion of granular materials with different basal resistance terms

different basal resistance terms. It is known that the kinetic energy starts to increase due to the gravity driven, and then to decreases when the influence of basal friction force exceeds the gravity force. The areas of energy change rate are the decrement or increment of energy during a time step, the kinetic energies of initial and final conditions both equal zero, thus, the areas of kinetic energy between the positive and negative regions are equal. It should be noted that the potential and dissipative energies keep negative or positive work. As similar with energy exchange laws, the energy change rate laws are very close between the Coulomb and Voellmy models.

The continuum assumption is not accurate in the instances that individual particles rolled along the bed and over each other proposed by Savage and Hutter (1989). The energies show significant changes when the moving time range from 3.0 to 5.0, i.e., the dynamical processes of granular materials moving from inclined plane to horizontal plane. Three basal resistance terms are adopted to simulate the motion of granular flow in the paper, and all models show excellent agreement with the experiment results. The energy exchanges and energy change rates, however, show apparent differences for VDFM by comparisons with the other models. It is a really challenge to describe the physical mechanisms of granular materials, especially for the natural rock avalanches and landslides.

6. Conclusions

Depth-averaged equations are widely used to simulate the motion of granular flows, basal resistance terms play an important role for the flow characteristics. Several typical basal resistance terms are summarized, and their effects on the key parameters in the motion such as runout distances and travel times are analyzed by performing the numerical simulations.

Numerical results for Coulomb model indicate that the bed friction angle significantly influences the dynamic characteristics such as runout distance, moving time. Similar founding was reported by Hutter *et al*. (1995) and Hungr (2008). Meanwhile, both the internal and basal angles have remarkable influences on earth pressure coefficient and the profile shape of granular materials.

For Voellmy model, the predicted results of rock avalanche and landslide conducted by Hungr and Evans (1996) and Chen and Lee (2003) performs quite well, except for several notable exceptions, but the predicted position heights are unrealistic (McClung and Mears 1995). Numerical results show the front and rear end positions, runout distances and moving times increase with increasing turbulent coefficient, the higher value of turbulent coefficient than reality may obtain more reasonable predicted runout for the small-scale avalanche or granular flow.

The simple Coulomb friction law may reflect the complex flow characteristics, especially for a thin layer steady flow, two friction coefficients of critical angle fitted by experiments are adopted in VDFM. We found that the effect of earth pressure coefficients on the motion of granular flow cannot be ignored, although it has moderate influence on the runout distance and moving time of granular flow. The numerical models with hydrostatic-isotropic assumption has a deeper profile at the rear end than that of Coulomb model. Although the moving time and runout distances of three basal resistance terms are very close, the energy exchange laws show that the flow characteristics have apparent differences between them, especially for VDFM.

Acknowledgments

Special thanks to two reviewers for their helpful comments on an earlier draft of this paper. This work was supported by the National Natural Science Foundation of China (51309262, 41472293 and 41472325), Scientific Research Foundation for the Introduction of Talent and Key Project of Chongqing Three Gorges University (14ZD17), the open project of State Key Laboratory Breeding Base of Mountain Bridge and Tunnel Engineering (CQSLBF-Y15-3), Programs for Science and Technology Development of Wanzhou district, Chongqing city (201203035) and Chinese National Committee for Integrated Research on Disaster Risk (IRDR2012-Y01).

References

Bagnold, R.A. (1954), "Experiments on a gravity-free dispersion of large solid spheres in a Newtonian fluid under shear", *Proc. R. Soc. London, Ser. A.*, **225**(1160), 49-63.

Camassa, R. and Holm, D.D. (1993), "An integrable shallow water equation with peaked solitons", *Phys. Rev. Lett.*, **71**(11), 1661.

Chen, H. and Lee, C.F. (2003), "A dynamic model for rainfall-induced landslides on natural slopes", *Geomorphology*, **51**(4), 269-288.

Chen, G.Q., Li, T.B. and He, Y.H. (2012), "Formation mechanism of groundwater for the land subsidence", *Res. J. Chem. Environ.*, **16**(s2), 56-62.

Chen, G.Q., Huang, R.Q., Xu, Q., Li, T.B. and Zhu, M.L. (2013a), "Progressive modelling of the gravity-induced landslide using the local dynamic strength reduction method", *J. Mt. Sci-Engl.*, **10**(4), 532-540.

Chen, G.Q., Li, T.B., Gao, M.B., Chen, Z.Q. and Xiang, T.B. (2013b), "Deformation warning and dynamic control of dangerous disaster for large underground caverns", *Disaster Adv.*, **6**(s1), 422-430.

Delinger, R.P. and Iverson, R.M. (2001), "Flow of variably fluidized granular masses across three-dimensional terrain: 2. Numerical predictions and experimental tests", *J. Geophys. Res.*, **106**(B1), 553-566.

Domnik, B. and Pudasaini, S.P. (2012), "Full two-dimensional rapid chute flows of simple viscoplastic granular materials with a pressure-dependent dynamic slip-velocity and their numerical simulations", *J. Non-Newtonian Fluid Mech.*, **173-174**, 72-86.

Domnik, B., Pudasaini, S.P., Katzenbach, R. and Miller, S.A. (2013), "Coupling of full two-dimensional and depth-averaged models for granular flows", *J. Non-Newtonian Fluid Mech*., **201**, 56-68.
Fei, M., Sun, Q., Zhong, D. and Zhou, G.G. (2012), "Simulations of granular flow along an inclined plane using the Savage-Hutter model", *Particuology*, **10**(2), 236-241.
Fernández-Nieto, E.D., Bouchut, F., Bresch, D., Castro Díaz, M.J. and Mangeney, A. (2008), "A new Savage–Hutter type model for submarine avalanches and generated tsunami", *J. Comput. Phys*., **227**(16), 7720-7754.
Fischer, J.T., Kowalski, J. and Pudasaini, S.P. (2012), "Topographic curvature effects in applied avalanche modeling", *Cold Reg. Sci. Technol*., **74**, 21-30.
Gray, J.M.N.T., Wieland, M. and Hutter, K. (1999), "Gravity-driven free surface flow of granular avalanches over complex basal topography", *Proc. R. Soc. London, Ser. A*., **455**(1985), 1841-1874.
Hungr, O. (2008), "Simplified models of spreading flow of dry granular material", *Can. Geotech. J*., **45**(8), 1156-1168.
Hungr, O. and Evans, S.G. (1996), "Rock avalanche runout prediction using a dynamic model", *Proceedings of the 7th International Symposium on Landslides*, Trondheim, Norway, June.
Hungr, O. and McDougall, S. (2009), "Two numerical models for landslide dynamic analysis", *Comput. Geosci*., **35**(5), 978-992.
Hutter, K. and Schneider, L. (2010), "Important aspects in the formulation of solid–fluid debris-flow models. Part II. Constitutive modelling", *Continuum Mech. Thermodyn*., **22**(5), 391-411.
Hutter, K., Savage, S.B. and Nohguchi, Y. (1989), "Numerical, analytical, and laboratory experimental studies of granular avalanche flows", *Ann. Glaciol*., **13**, 109-116.
Hutter, K., Koch, T., Pluüss, C. and Savage, S.B. (1995), "The dynamics of avalanches of granular materials from initiation to runout. Part II. Experiments", *Acta Mech*., **109**(1-4), 127-165.
Iverson, R.M. (1997), "The physics of debris flows", *Rev. Geophys*., **35**(3), 245-296.
Iverson, R.M. and Denlinger, R.P. (2001), "Flow of variably fluidized granular masses across three-dimensional terrain: 1. Coulomb mixture theory", *J. Geophys. Res*., **106**(B1), 537-552. DOI: 10.1029/2000JB900329
Johnson, C.G. and Gray, J.M.N.T. (2011), "Granular jets and hydraulic jumps on an inclined plane", *J. Fluid Mech*., **675**, 87-116.
Li, X., He, S., Luo, Y. and Wu, Y. (2012), "Simulation of the sliding process of Donghekou landslide triggered by the Wenchuan earthquake using a distinct element method", *Environ. Earth Sci*., **65**(4), 1049-1054.
McClung, D.M. and Mears, A.I. (1995), "Dry-flowing avalanche run-up and run-out", *J. Glaciol*., **41**(138), 359-372.
Ouyang, C., He, S., Xu, Q., Luo, Y. and Zhang, W. (2013), "A MacCormack-TVD finite difference method to simulate the mass flow in mountainous terrain with variable computational domain", *Comput. Geosci*., **52**, 1-10.
Pirulli, M., Bristeau, M.O., Mangeney, A. and Scavia, C. (2007), "The effect of the earth pressure coefficients on the runout of granular material", *Environ. Modell. Softw*., **22**(10), 1437-1454.
Pitman, E.B. and Le, L. (2005), "A two-fluid model for avalanche and debris flows", *Phil. Trans. R. Soc. A*, **363**(1832), 1573-1601.
Pitman, E.B., Nichita, C.C., Patra, A., Bauer, A., Sheridan, M. and Bursik, M. (2003), "Computing granular avalanches and landslides", *Phys. Fluids*, **15**(12), 3638-3646.
Pouliquen, O. (1999a), "On the shape of granular fronts down rough inclined planes", *Phys. Fluids*, **11**(7), 1956-1958.
Pouliquen, O. (1999b), "Scaling laws in granular flows down rough inclined planes", *Phys. Fluids*, **11**(3), 542-548.
Pouliquen, O. and Forterre, Y. (2002), "Friction law for dense granular flows: application to the motion of a mass down a rough inclined plane", *J. Fluid Mech*., **453**, 133-151.
Pudasaini, S.P. (2012), "A general two-phase debris flow model", *J. Geophys. Res*., **117**(F3). DOI: 10.1029/2011JF002186

Pudasaini, S.P. (2014), "Dynamics of submarine debris flow and tsunami", *Acta Mech*., **225**(8), 2423-2434.
Pudasaini, S.P. and Domnik, B. (2009), "Energy considerations in accelerating rapid shear granular flows", *Nonlinear Proc*. *Geoph*., **16**(3), 399-407.
Pudasaini, S.P. and Hutter, K. (2007), *Avalanche Dynamics*: *Dynamics of Rapid Flows of Dense Granular Avalanches*, Springer, New York, NY, USA.
Pudasaini, S.P. and Krautblatter, M. (2014), "A two-phase mechanical model for rock-ice avalanches", *J*. *Geophys*. *Res*. *Earth Surf*., **119**(10), 2272-2290.
Pudasaini, S.P. and Kröner, C. (2008), "Shock waves in rapid flows of dense granular materials: Theoretical predictions and experimental results", *Phys*. *Rev*. *E*, **78**(4), 041308.
Pudasaini, S.P., Wang, Y. and Hutter, K. (2005a), "Modelling debris flows down general channels", *Nat*. *Hazard*. *Earth*. *Sys*., **5**(6), 799-819.
Pudasaini, S.P., Hsiau, S.S., Wang, Y. and Hutter, K. (2005b), "Velocity measurements in dry granular avalanches using particle image velocimetry technique and comparison with theoretical predictions", *Phys*. *Fluids*, **17**(9), 093301.
Salm, B. (1993), "Flow transition and runout distances of flowing avalanches", *Ann*. *Glaciol*., **18**, 221-226.
Savage, S.B. and Hutter, K. (1989), "The motion of a finite mass of granular material down a rough incline", *J*. *Fluid Mech*., **199**, 177-215.
Savage, S.B. and Hutter, K. (1991), "The dynamics of avalanches of granular materials from initiation to runout. Part I: Analysis", *Acta Mech*., **86**(1-4), 201-223.
Tai, Y.C., and Kuo, C.Y. (2008), "A new model of granular flows over general topography with erosion and deposition", *Acta Mech*., **199**(1-4), 71-96.
Tai, Y.C., Noelle, S., Gray, J.M.N.T. and Hutter, K. (2002), "Shock-capturing and front-tracking methods for granular avalanches", *J*. *Comput*. *Phys*., **175**(1), 269-301.
Teufelsbauer, H., Wang, Y., Pudasaini, S.P., Borja, R.I. and Wu, W. (2011), "DEM simulation of impact force exerted by granular flow on rigid structures", *Acta Geotech*., **6**(3), 119-133.
Thornton, A.R. (2005), "A study of segregation in granular gravity driven free surface flows", Ph.D. Dissertation; The University of Manchester, Manchester, England.
Toro, E.F. (2001), *Shock-capturing Methods for Free-surface Shallow Flows*, John Wiley and Sons, NJ, USA.
Tóth, G. and Odstrčil, D. (1996), "Comparison of some flux corrected transport and total variation diminishing numerical schemes for hydrodynamic and magneto hydrodynamic problems", *J*. *Comput*. *Phys*., **128**(1), 82-100.
Wang, X., Morgenstern, N.R. and Chan, D.H. (2010), "A model for geotechnical analysis of flow slides and debris flows", *Can*. *Geotech*. *J*., **47**(12), 1401-1414.
Yee, H. (1989), "A class of high resolution explicit and implicit shock capturing methods", NASA TM-101088.

CC